A Study of the Kinematics of the Local Dark Clouds*

B. Ramesh *Raman Research Institute, C. V. Raman Avenue, Sadashivanagar, Bangalore 560 080.*

Abstract. Lack of reliable estimates of distances to most of the local dark clouds has, so far, prevented a quantitative study of their kinematics. Using a statistical approach, we have been able to extract the average spatial distribution as well as the kinematical behaviour of the local dark clouds from their measured radial velocities. For this purpose, we have obtained radial velocities for 115 southern clouds and used the data from the literature for the northern ones. In this paper we present this new data, analyse the combined data and compare our results with those arrived at by earlier studies.

The local clouds are found to be expanding at a speed of $\sim 4\,\mathrm{kms}^{-1}$ which is in general agreement with the estimates from optical and HI studies. However, it is found that the kinematics of the local clouds is not described by the model proposed for the local HI gas where a ring of gas expanding from a point gets sheared by the galactic rotation. Rather, the observed distribution of their radial velocities is best understood in terms of a model in which the local clouds are participating in circular rotation appropriate to their present positions with a small expansion also superimposed. This possibly implies that cloud–cloud collisions are important. The spatial distribution of clouds derived using such a model is in good agreement with the local dust distribution obtained from measurements of reddening and extinction towards nearby stars. In particular, a region of size $\sim 350\,\mathrm{pc}$ in diameter enclosing the Sun is found to be devoid of clouds. Intriguingly, most clouds in the longitude range 100° to 145° appear to have negative radial velocities implying that they are approaching us.

Key words: Local ISM structure—Gould's belt—dispersion in cloud velocities.

1. Introduction

OB associations affect substantially the structure, the motion and the evolution of the surrounding interstellar medium over large scales. There are several examples of *shells* and *supershells* in our galaxy as well as in the Large Magellanic Cloud. These

---

are regions of low density gas surrounded by denser clouds, actively forming stars and often found to be expanding. Their sizes and energies seem to be consistent with their formation around OB associations due to the combined action of the ionising radiation, stellar winds and supernovae (Elmegreen 1991). The systematic non-circular motions thus caused will eventually get randomised through cloud–cloud collisions possibly mediated by galactic magnetic fields. These random motions play important roles in cloud-agglomeration (Kwan 1979) and stellar acceleration through gravitational scattering (Stark & Blitz 1978; Spitzer & Schwarzschild 1951). Studies of such regions around OB associations would, therefore, enable one to understand better the processes of large scale energy injection and its eventual redistribution as well as the significance of induced star-formation.

The solar system seems to be inside one such expanding cavity. The reddening measured towards nearby stars indicates that the dust in the solar neighbourhood is distributed in a shell (Lucke 1978) with the surrounding dense clouds harbouring the prominent local OB associations. The local OB stars are apparently confined to a plane inclined to the galactic disc at an angle of $\sim 18°$ forming the *Gould's belt* on the sky. They are found to be expanding with a velocity of $\sim 5\,\mathrm{kms}^{-1}$ (Cameron & Torra, 1990 and references therein). The local HI gas seems to have the kinematics of a thin ring which expands from a point at $\sim 4\,\mathrm{kms}^{-1}$ and gets sheared by the galactic rotation (Lindblad *et al.* 1973; Olano 1982). A recent study by Taylor *et al.* (1987) of the nearby dark clouds concluded that while these clouds are also expanding, their kinematics is not described well by the above model. The study by Taylor *et al.* was limited to clouds in the northern longitude range of 0° to 220°, especially to those assigned to Gould's belt using a simple proximity criterion. Hence, it was desirable to extend these observations to the rest of the longitude range, i.e. $220° \lesssim 1 \lesssim 360°$, to make a more complete study of the kinematics of the local clouds. Also, Taylor *et al.* could not estimate the expansion in various directions quantitatively owing to lack of reliable estimates of distances to most nearby clouds. This paper presents our attempt to improve the situation on both counts.

We carried out a CO survey of the southern clouds to obtain their radial velocities. Though the main motivation was to supplement the northern data, there was an additional reason: Whereas Kerr *et al.* (1981) found that the Lindblad's feature A which delineated *Gould's belt* in the northern sky was also present in the third quadrant upto $1 \sim 236°$, May *et al.* (1988) found that there was no evidence for a corresponding feature traced by molecular clouds in the southern CO survey. Thus it was important to make an independent study of the southern dark clouds to confirm whether there was a molecular counterpart to *Gould's belt* and the associated HI gas in the southern galaxy as well. We also undertook a detailed kinematic study of the local population of dark clouds, northern as well as southern. Using a novel approach based on statistical techniques, we have determined the average spatial distribution as well as the kinematical behaviour of the local dark clouds from their measured radial velocities. In this paper, we present the new data, our analysis of the new as well as existing data and compare our results with those arrived at by earlier studies.

In the next section, details of our observations and the measured velocities are presented. The analysis of the radial velocities of the local dark clouds is presented in section 3 at the end of which the main results are summarised. In section 4 these are discussed in relation to the conclusions of earlier workers.

2. Observations

A survey of the southern dark clouds in $J = 1 \rightarrow 0$ transition of ^{12}CO to obtain their radial velocities was carried out in February–April 1992 using the 10·4 m millimeterwave telescope operated by Raman Research Institute, Bangalore (for a brief description of the telescope, see Patel 1990). A filter-bank spectrometer with 250 kHz (0·65 kms^{-1}) resolution covering a total bandwidth of 64 MHz was used. Pointing was checked by beam-switched continuum scans on Jupiter (see Patel 1990 for details). An ambient temperature load was used for calibration. During the observations, the DSB T_{sys} ranged from 600 K to 1100 K. Frequency switching by 15·25 MHz was used for all the observations and the spectra obtained were appropriately combined to recover the loss in S/N due to the switching. Third order polynomials were fitted to the spectra to estimate and remove the curved baselines.

The clouds observed were selected from the catalogue of southern dark clouds compiled by Feitzinger & Stuwe (1984). Their opacity class (mostly > 2) and declination were the criteria used for the selection. Of the 149 clouds observed only 115 were detected in CO. The reason for the non-detection of a large fraction (23%) of the clouds is not entirely clear but may partly be due to our relatively higher detection limit ($3\sigma \sim 1$ K). Table 1 (a) and 1 (b) list the co-ordinates of the clouds detected and their radial velocities obtained by fitting gaussians to the spectral components. The estimated rms error on the velocities is ~ 0.3 kms^{-1}. Table 2 gives a longitudinal sector-wise break-up of the number of dark clouds, with opacity class > 2, listed in the catalogue of Feitzinger and Stuwe, and of those observed and detected by us. Only 30% of the clouds in the longitude range 280° to 320° were accessible from our site.

3. Kinematical analysis and simulations

The kinematical analysis of the local dark clouds presented in this section consists of three parts: (i) The clouds around the four directions 0, 90, 180 and 270 degrees, which we will henceforth refer to as *null* directions, are analysed to estimate the magnitudes of the systematic and random components of their non-circular motions. In general, to estimate these components the contributions due to the circular rotation of the galaxy must be removed first. However, for nearby ($\lesssim 1$ kpc) clouds these contributions are expected to be zero in these four special directions and small for the neighbouring longitudes. So, lack of knowledge of the distances to the clouds around these four directions is not a handicap. (ii) To find if the motions found in (i) are more general, a subset of clouds with reliable estimates of distances and distributed over all longitudes is analysed. (iii) The non-circular motions are quantified independently from an analysis of the radial velocities towards the general population of clouds distributed in all longitudes using statistical techniques and a model for their spatial distribution. Consequently, a *probable* spatial distribution for the clouds is also obtained.

Before describing the three parts of the analysis we wish to make the following remarks:

■ The distribution of the clouds in the plane of the sky is shown in Fig. 1a. The
  double sinusoidal behaviour seen in their longitude-velocity plot (Fig. 1b) clearly

Table 1a. Lists the coordinates of the southern dark clouds detected in CO taken from the catalogue of Feitzinger & Stuwe (1984) and their radial velocities obtained by fitting gaussians to the spectra. The serial number in their catalogue is given as the cloud number. The clouds are ordered in galactic longitude and latitude.

Cloud	l^{II}	b^{II}	V_{lsr}	Cloud	l^{II}	b^{II}	V_{lsr}
002	237.40	−2.89	25.4	098	270.10	−0.28	1.2
004	237.40	−4.86	20.7	101	270.50	−1.75	4.7
009	239.40	−4.70	23.4	105	270.90	2.48	−3.5
012	247.00	−0.61	20.9	109	271.40	4.89	−3.2
013	247.30	−2.79	−23.4	111	272.50	−3.93	5.4
018	250.30	0.25	12.5	111A	275.30	−1.11	−4.8
024	253.10	−4.28	11.4	114	274.60	0.13	−2.2
025	253.10	−1.37	10.4	116	275.50	2.14	−6.2
026	253.30	3.30	6.7	118	276.30	−0.68	−3.9
030	255.40	−4.88	9.3	142	285.20	9.44	5.7
031	255.50	−4.20	9.8	152	287.80	7.66	4.7
032	255.80	−2.71	9.4	152A	287.80	7.67	10.9
036	258.10	−3.15	−20.4	163	291.00	7.82	8.2
040	259.00	0.96	6.0	163A	291.10	7.85	6.3
041	259.20	3.35	6.9	206	301.70	7.63	13.5
042	259.30	−13.26	4.8	228	304.00	7.37	14.5
044	259.50	−16.54	−21.4	243	307.10	6.54	−13.7
046	259.80	−2.59	9.1	249	308.40	5.81	−2.3
049	260.60	−3.63	6.2	259	311.10	5.79	18.2
050	260.60	−3.70	5.5	262	311.60	−1.18	−1.8
055	262.20	−12.46	5.2	277	315.90	5.90	6.0
056	262.40	3.12	9.0	278	316.10	4.94	−3.1
058	263.10	1.35	6.3	293	319.70	1.53	−17.3
071	265.90	−7.53	3.3	302	323.10	−0.96	−6.0
072	266.00	−7.63	3.3	305	323.80	5.59	−20.2
075	266.70	4.93	2.6	311	326.30	−0.58	−17.3
080	267.30	0.04	4.8	316	331.80	1.82	27.3
081	267.50	4.30	1.0	320	334.30	−1.01	−11.3
082	267.60	−7.35	5.4	321	334.60	18.09	5.8
085	268.10	1.82	−0.5	327	335.30	3.15	3.4
087	268.50	−1.74	1.7	328	335.40	−1.14	−11.8
091	269.40	−7.57	4.8	332	336.10	−2.31	−12.1
093	269.80	4.02	−3.0	333	336.30	3.94	31.5
094	269.80	−11.10	0.1	334	336.40	11.31	6.5
096	270.00	2.88	−2.7	336	336.50	19.14	6.0

Table 1a. (continued)

Cloud	lII	bII	V_{lsr}	Cloud	lII	bII	V_{lsr}
337	336.80	−0.96	−21.8	418	354.90	14.97	3.4
339	337.00	4.84	4.1	419	354.90	16.00	2.5
341	337.40	16.68	5.0	429	357.20	4.40	6.4
348	338.90	9.50	6.1	431	357.30	0.90	1.7
349	339.00	16.16	4.9	439	358.60	15.37	2.5
365	342.10	−3.72	−15.7	441	358.90	−3.90	5.2
383	346.70	−9.72	4.9	446	359.80	−18.31	5.3
392	347.90	3.16	−2.9	450	0.22	−18.73	4.7
395	348.80	3.57	2.2	453	1.07	−20.52	4.9
398	350.60	2.60	6.1	456	1.44	9.38	3.5
403	352.00	16.31	3.9	464	3.67	6.35	4.3
406	352.60	1.02	5.5	473	6.11	−1.22	13.4
408	352.80	17.85	2.8	476	6.69	−0.55	−102.5
411	353.60	15.78	4.0	477	6.84	−2.15	10.8
414	354.30	16.35	2.2	479	7.09	−2.32	9.4
415	354.50	−1.70	3.4				

Table 1b. Similar to Table 1a, but for lines-of-sight with double components. The velocity of the stronger one is given first followed by that of the weaker one.

Cloud	lII	bII	$V_{lsr}(1)$	$V_{lsr}(2)$
006	238.40	−4.12	20.5	18.9
007	238.90	−1.57	19.1	27.1
022	251.90	−3.16	13.1	18.3
038	258.60	−2.69	9.5	17.8
052	261.60	0.33	10.9	5.3
053	261.70	−4.36	10.0	13.5
064	265.10	1.43	5.2	8.1
067	265.40	0.41	5.9	0.0
078	267.00	−0.94	4.4	7.7
090	269.40	−1.34	4.0	8.2
099	270.20	−0.98	0.6	6.1
102	270.50	0.53	6.6	−0.2
122	277.10	−2.56	−6.7	−2.0
134	281.60	−0.81	−3.4	3.8
145	286.20	0.10	−20.0	−8.6
149	287.20	−0.21	−18.5	−7.6
342	338.00	16.58	5.2	6.8
372	344.00	−0.41	37.0	33.7

388	347.00	0.51	6.1	-9.8
400	350.80	1.00	5.7	-5.4
406	352.60	1.00	5.5	-1.1
407	352.70	0.90	2.6	5.7
409	352.90	16.93	3.2	2.4
421	355.10	1.60	7.1	-1.9
435	357.90	-2.00	-0.5	4.3
445	359.60	-17.75	6.1	3.6
449	0.21	-4.52	8.7	5.7

Table 2. Observation and detection statistics.

Longitude range	Number of clouds	Observed	Detected	Observed %	Detected %
240°-280°	80	69	53	86.3	76.8
280°-320°	57	17	11	29.8	64.7
320°-360°	99	63	51	63.6	81.0

shows that the contribution of galactic differential rotation is important. We estimate these contributions using the equation

$$V_{rot}(l) = Ad\sin(2l) \tag{1}$$

with a value of $14\cdot5\,\mathrm{kms^{-1}\,kpc^{-1}}$ for Oort's constant A. Here d is the distance and l is the longitude of the cloud. We have omitted a factor $\cos^2 b$ in this equation because most of the clouds have latitudes $|b| < 20°$ (Fig. 1a) making the correction unimportant.

■ We shall consider each *condensation* of $1\cdot5°$ extent in longitude and latitude, and $2\,\mathrm{kms^{-1}}$ width in velocity, as a *distinct kinematical entity*. The angular size was chosen to be $1\cdot5°$ because at a distance of 400 pc, the mean distance of these dark clouds as suggested by Feitzinger & Stuwe (1986), the corresponding linear size would be 10 pc which is the upper end of the sizes of these dark clouds under study. Hence we convolved the measured points with a 3-dimensional gaussian of full width at half maximum in each of the three dimensions equal to the values mentioned above and picked all the local peaks. All points thus obtained are treated as *independent clouds* and used in the following analysis.

■ A few clouds with absolute velocities more than $25\,\mathrm{kms^{-1}}$ have been excluded from our analysis. As we shall see, the magnitudes of the systematic and peculiar components of non-circular velocities of the local clouds turn out to be $\sim 4\,\mathrm{kms^{-1}}$, and hence these few clouds, are likely to be far away and can safely be excluded.

3.1 Clouds in the null directions

To get a statistically significant number of clouds around each of the four *null* directions for the present analysis we include all the clouds within a longitude
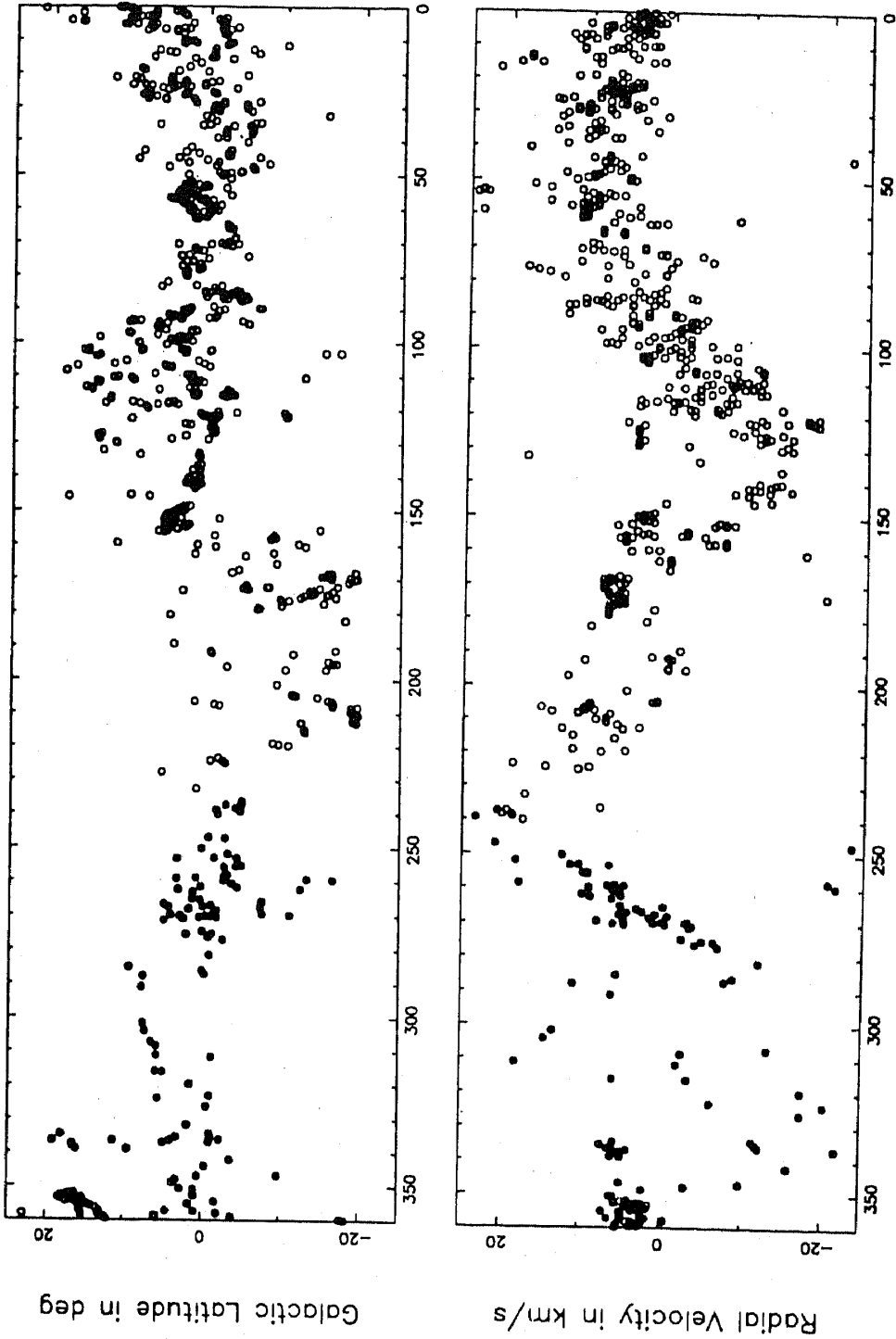
Figure 1. The upper panel (a) shows the latitude *vs* longitude plot for the entire population of clouds. The lower panel (b) shows the distribution of their radial velocities at different longitudes. In both the plots, the filled circles represent the southern clouds observed by us, while the open ones refer to the northern clouds detected by Taylor *et al.* (1987).

strip of 18° centered around them. We correct for the small contributions to their radial velocities from differential rotation by adopting a mean distance to the clouds in each group. The adopted distances are based on the proximity in the sky and in velocity of these clouds to the reflection nebulae with reasonably good estimates of distances. These distances are also found to be in reasonable agreement with the estimates from the slopes of the distributions of each group of clouds in longitude-velocity plots. The adopted distances for the four groups around the directions 0, 90, 180 and 270 are 180, 500, 140 and 450 pc respectively. We have adopted a distance of 350 pc for a small sub-group of clouds in the 180° direction distinct from the Taurus group of clouds. Similarly, for a sub-group of clouds in the 270° direction that does not trace the Vela IRAS shell found by Sahu (1992) and lies close to the plane coincident with the Vela Molecular Ridge we have adopted a distance of 1·2 kpc. We have also excluded a small sub-group of clouds around the 0° direction lying in the longitude range of 3° to 6° latitude range of $-1°$ to $-2·5°$ with a mean velocity of $10·5 \, \mathrm{kms}^{-1}$ from the analysis. This is because they are likely to be at 900 pc as indicated by their proximity in the sky and in velocity to a reflection nebula at that distance.

After correction for differential rotation on the above basis, the left over errors will be only due to the dispersion in distances. Even if the dispersion in distance about the mean value is as much as the mean distance itself, i.e. ~ 400 pc, the maximum error in the correction at either edge of the strip is $\sim 1 \, \mathrm{kms}^{-1}$ and the average error will be much less. Since this is comparable to the measurement errors in velocity and negligible compared to the dispersion in velocities, including all clouds within a longitude strip of 18° around the *null* directions for the present analysis is justified.

The distribution of residual velocities after these corrections, shown in Fig. 2, were fitted with Gaussians. The mean and the standard deviation give the magnitude of the systematic and the random components of the non-circular motions and are listed in Table 3. In the case of longitudes 180° and 270°, two sets of parameters corresponding to the two distinct groups in each direction are given separately. From these results, we conclude that receding motions of 3 to $6 \, \mathrm{kms}^{-1}$ are present in all of them. However, in three of the four directions the samples are dominated by specific groups of clouds and hence their receding motions are not necessarily conclusive evidence for general expansion of the local dark clouds. This we proceed to check in the next sub-section. The magnitude of the velocity dispersion of clouds is ~ 2 to $5 \, \mathrm{kms}^{-1}$, much lower than 7 to $10 \, \mathrm{kms}^{-1}$ derived by Stark (1984) and we discuss this issue in section 4.

Table 3. Results of *null* direction analysis.

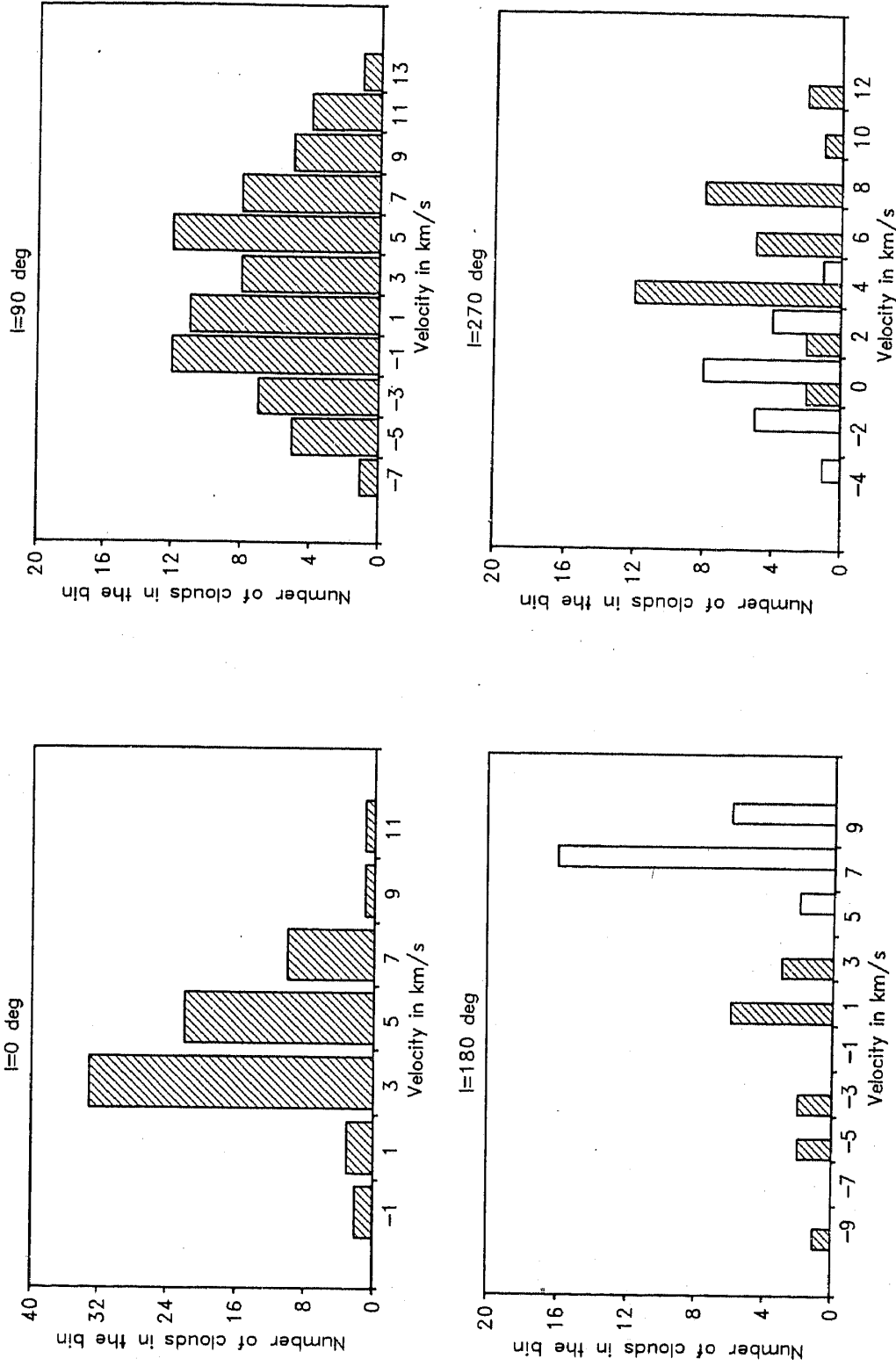| Longitude bins	$V_{exp}(\mathrm{kms}^{-1})$	$\sigma(\mathrm{kms}^{-1})$	Comments
0	4.6	2.0	Ophiuchus group of clouds.
90	2.7	5.0	
180	6.3	1.3	Taurus group of clouds.
	0.3	3.6	
270	6.5	3.0	Vela IRAS shell.
	0.0	1.5	

Figure 2. The filled bars in the four panels show the distribution of the residual velocities of the clouds in the four *null* directions. Their LSR velocities have been corrected for adopted distances of 180, 500, 140 and 450 pc respectively. Oort's A constant was taken to be 14·5 kms^{-1} kpc^{-1}. The empty bars in the 180° and 270° directions represent clouds associated with the Taurus group at ∼150 pc and the Vela Molecular Ridge at ∼1200 pc respectively.

B. Ramesh

Table 4. Reflection nebulae nearer than 500pc.

Cloud	l deg	b deg	Dist kpc	V_{LSR} kms^{-1}	V_{res} kms^{-1}
vdB124	21.0	−0.5	0.17	6.9	5.3
vdB123	31.6	5.2	0.44	7.2	1.5
vdB129	41.6	−18.1	0.04	0.1	−0.5
vdB126	57.0	3.0	0.48	11.7	5.3
vdB135	73.5	−5.1	0.35	12.4	9.6
vdB136	81.4	0.5	0.40	8.5	6.8
vdB147	94.3	−5.3	0.44	6.7	7.7
vdB152	110.3	11.4	0.40	−5.3	−1.5
vdB158	110.6	−12.6	0.48	−8.1	−3.5
vdB150	111.9	14.1	0.50	−4.0	1.0
vdB003	121.4	6.6	0.18	−6.8	−4.5
vdB007	132.9	9.1	0.08	−13.3	−12.1
vdB008	133.9	7.6	0.21	−11.6	−8.6
vdB012	157.4	−20.6	0.17	1.1	2.8
vdB013	158.0	−21.3	0.29	7.0	9.9
vdB017	158.3	−20.4	0.50	7.2	12.2
vdB016	159.2	−21.9	0.14	5.3	6.6
vdB019	160.5	−17.8	0.30	8.6	11.3
vdB032	162.5	1.5	0.30	−2.4	0.1
vdB025	171.4	−19.8	0.11	11.1	11.6
vdB029	172.1	−9.7	0.15	6.4	7.0
vdB034	172.1	−2.3	0.32	6.8	8.1
vdB031	172.5	−0.8	0.12	6.2	6.7
vdB041	182.5	−5.9	0.16	7.7	7.5
vdB056	190.5	−6.9	0.26	8.9	7.5
vdB038	194.6	−15.6	0.32	0.5	−1.8
vdB040	196.8	−15.7	0.24	−5.4	−7.3
vdB043	198.1	−14.6	0.38	−10.3	−13.6
vdB044	207.8	−19.7	0.55	11.1	4.5
vdB055	212.4	−19.0	0.38	2.7	−2.3
vdB087a	221.8	−2.0	0.50	39.8	32.6
vdB086	222.7	−3.4	0.42	11.9	5.8
vdB090a	224.4	−2.7	0.52	14.1	6.6
vdB098	240.4	−2.2	0.38	23.0	18.3
vBH10a	259.3	−3.8	0.48	8.9	6.4
vBH28	265.1	1.4	0.50	5.2	4.0
vBH12	266.2	−7.8	0.48	3.3	2.4
vBH23	267.0	−0.9	0.46	4.5	3.8
vBH63	314.9	−5.1	0.42	4.8	10.9
vdB105	352.9	17.0	0.17	3.6	4.2
vdB108	353.1	15.9	0.14	4.5	5.0
vdB106	353.7	17.7	0.14	2.3	2.7
vdB100a	354.6	22.7	0.15	5.1	5.5
vdB102x	355.5	20.9	0.13	3.3	3.6

Table 4. (continued) Reflection nebulae farther than 500pc

Cloud	l	b	Dist	V_{LSR}	$V_{...}$
	deg	deg	kpc	km s^{-1}	km s^{-1}
vdB115	7.4	−1.8	0.91	8.9	
vdB128	69.5	0.4	0.83	−2.2	
vdB131x	80.5	2.7	1.05	5.0	
vdB142	99.1	3.9	0.72	−8.2	
vdB155	109.6	2.4	0.58	−9.5	
vdB001c	117.3	−3.7	0.52	−11.4	
vdB002	119.0	3.0	0.63	−19.5	
vdB014	141.5	2.9	0.76	7.6	
vdB039	174.3	−1.7	0.72	7.4	
vdB047	184.0	−4.2	0.87	3.0	
dB075	188.7	3.8	0.55	3.0	
vdB077x	201.9	0.0	1.00	0.0	
vdB051	206.0	−16.3	0.66	9.8	
vdB057	207.1	−16.2	0.58	9.8	
vdB068x	213.7	−12.4	0.76	9.5	
vdB080a	219.3	−9.0	0.76	12.6	
vdB093	223.7	−1.9	0.72	17.9	
vdB095	224.7	−1.8	0.79	15.6	
vdB094	225.5	−2.6	0.83	12.4	
vBH05	253.1	−1.4	1.32	10.4	
vBH03	255.5	−4.2	1.15	9.9	
vBH04	255.6	−3.0	0.87	8.9	
vBH17	260.0	−0.1	0.95	7.8	
vBH27	264.3	1.9	0.91	7.0	
vBH25b	264.4	1.4	0.60	6.3	
vBH29	268.0	1.8	0.79	−0.5	
vBH30	270.8	0.8	0.95	6.9	
vBH72	336.4	−1.4	1.38	−12.4	
vBH92	358.5	−2.1	1.32	−0.5	

3.2 *Clouds with known distances*

Here, we analyse two sets of clouds: first, those with associated reflection nebulae and second those identified as *individual* by Dame *et al.* (1987) from the composite CO survey.

Reliable estimates of distances to many clouds with associated reflection nebulae already exist. Racine (1968) has obtained the distances to the northern reflection nebulae while van den Bergh & Herbst (1975) have obtained distances for the southern ones. The velocities for the northern clouds have been reported by Kutner *et al.* (1980) and for the southern ones by de Vries *et al.* (1984). For a few clouds for which the data did not exist, we have obtained the radial velocities using the $J = 1 \rightarrow 0$ transition of carbon monoxide. Quantities relevant to our discussion have been taken from the literature and summarized in Table 4. The table lists the clouds with

Figure 3. The spatial distribution of clouds with reflection nebulae projected onto the galactic plane. The heads of the *tadpoles* indicate the position of the clouds, while the lengths of the *tails* indicate the magnitude of their residual velocities. Clouds with outward radial velocities are indicated by filled squares, and those coming in by filled circles. The sun is located at the centre of the system of concentric circles. Notice that the clouds in the longitude ranges 100°–145° and 195°–215° are predominantly moving inward.

associated reflection nebulae, both northern (names with 'vdB' as prefix) and southern (names with 'vBH' as prefix), their longitudes, latitudes, distances and LSR and residual velocities.

There are 44 clouds within 500 pc and 29 beyond that have associated reflection nebulae. Fig. 3 shows the spatial distribution of their residual velocities projected onto the plane of the Galaxy with the Sun at the origin and the galactic centre towards the negative Y-axis. The clouds within 500 pc show a clear trend of expansion with a mean velocity of $\sim 4.3\,\mathrm{kms}^{-1}$ and a dispersion of $\sim 7\,\mathrm{kms}^{-1}$ while those outside 500 pc show only marginal evidence for expansion. Notice that the clouds in the longitude range 100° to 145° and possibly in the range 195° to 215° form a *distinct kinematical group* with predominantly 'in coming' velocities. They have the effect of reducing the mean expansion velocity and increasing the apparent dispersion. After removing the clouds in these two sectors, there are 33 clouds within 500 pc and 20 beyond. The distribution of their residual velocities is shown in Fig. 4. The filled rectangles represent clouds within 500 pc and the empty ones refer to the clouds beyond. Now, the expansion velocity for the clouds within 500 pc is $7.2\,\mathrm{kms}^{-1}$ with a standard deviation for the random velocities of $5.8\,\mathrm{kms}^{-1}$. Clouds outside 500 pc show $2.3\,\mathrm{kms}^{-1}$ expansion with $4\,\mathrm{kms}^{-1}$ random velocity dispersion. One may thus firmly conclude that the clouds within 500 pc show clear evidence of expansion of $\sim 7\,\mathrm{kms}^{-1}$ in all longitudes except the longitude ranges 100° to 145° and 195° to 215° where most of the clouds have negative velocities. Those outside 500 pc also show expansion, although marginal.

Now we turn to the analysis of the second set of clouds. Dame *et al.* (1987) have identified clouds and cloud complexes within 1 kpc from the composite CO survey. In general, these complexes have large angular extent. In Table 2 of their paper, Dame *et al.* have listed these clouds, their longitude and latitude ranges, their measured radial velocities and their distances compiled from the literature. These distances are
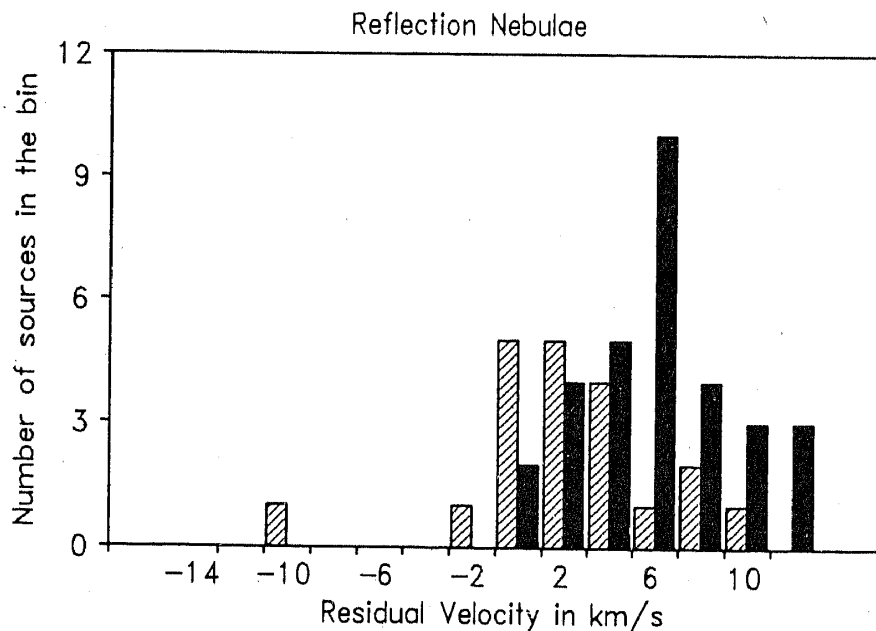
Figure 4. A histogram of the residual velocities of the clouds with associated reflection nebulae excluding those in the longitude ranges 100°–145° and 195°–215°. Filled bars correspond to clouds within 500 pc while those beyond 500 pc are denoted by hatched bars.

Table 5. Composite CO survey clouds.

Cloud	l deg.	b deg.	V_{LSR} kms^{-1}	Dist. kpc	V_{res} kms^{-1}
ρ Ophiuchus	0.5	7.8	3.0	165	3.0
R CrA	0.5	−18.0	6.0	150	6.0
Aquila rift	26.3	2.0	8.0	200	5.7
Aquila rift	39.0	0.0	8.0	200	5.2
Cloud B	49.0	0.5	7.0	300	2.7
Vulpecula rift	58.5	1.0	10.0	400	4.8
Cepheus	110.0	16.5	−5.0	450	−1.1
Lindblad ring	132.0	3.0	1.0	300	5.3
Perseus 2b	158.3	−16.0	5.0	350	8.2
Perseus 2a	167.0	−7.5	−3.0	350	−0.8
Taurus	170.5	−15.8	5.0	140	5.6
Orion B	205.3	−13.5	8.0	450	3.2
Orion A	213.3	−17.8	8.0	450	2.6
Vela sheet	275.5	2.5	3.0	400	4.1
Chamaleon	300.0	−16.0	4.0	215	6.5
Coal sack	303.5	−0.5	−4.0	175	−1.7
G317−4	317.5	−4.0	−6.0	170	−3.6
Lupus	339.5	13.0	5.0	170	6.5
ρ Ophiuchus	356.0	18.5	3.0	165	3.3

based on associated Population I objects or on star counts or on the relation of visual absorption to distance for stars within the cloud boundary. Here we analyze the radial velocities of clouds within 500 pc. The quantities relevant to our discussion are summarized in Table 5. We have used 8 kms^{-1} and 3 kms^{-1} as the velocities of the Orion and Vela clouds respectively. The longitudes and latitudes listed in Table 5 are the averages of the boundary values given by Dame et al.. A histogram of the residual velocities is shown in Fig. 5. The mean velocity of expansion is $\sim 3\cdot5$ kms^{-1}, with a dispersion in the cloud velocities of ~ 3 kms^{-1}. We realise that these clouds have large spatial extent and any analysis which assigns a single position, distance and LSR velocity (as done here) is bound to be inaccurate. It is significant that in spite of the possible scatter introduced by this assumption this analysis also leads us to the same conclusions as before, viz. that the local clouds are in a state of expansion.

3.3 The general population of clouds

Having found that 'null' direction clouds as well as clouds with known distances and distributed over the entire longitude range show evidence of expansion of ~ 3 to 5 kms^{-1} and a velocity dispersion of 2 to 5 kms^{-1}, we set out to examine whether this apparent expansion about a common centre is true for the entire population of the local clouds. In the process, we have also derived their average spatial distribution. For this analysis, we divided the local cloud population into 10 groups in the following way: In each of the four quadrants in longitude we exclude clouds
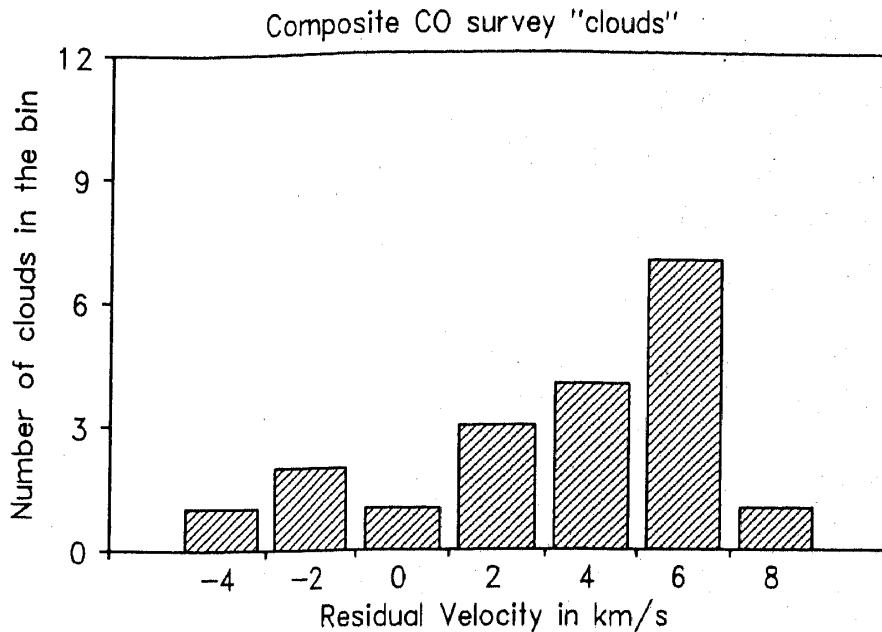
Composite CO survey "clouds"

Figure 5. A histogram of the residual velocities of the *CO survey clouds.*

within $15°$ from the null directions since there is not much distance information that can be derived in these directions. Thus, within each quadrant only clouds within the central $60°$ are considered. In the first 3 quadrants these $60°$ segments are further divided into three sectors of $20°$ each. However, since the total number of clouds in the fourth quadrant is only 25, we analyse them as one single group. Thus the sample included in the present analysis is divided into 10 groups.

Clouds in each group were then subjected to an analysis procedure that involves the following two steps: (1) To generate the positions and radial velocities of pseudo-clouds, same in number as the actual ones, using Monte-Carlo simulations, assuming a model for their spatial distribution (described below). (2) To determine the probability that the simulated cloud velocities and the actually measured cloud velocities are drawn from the same parent distribution using a statistical test. These two steps are repeated for various sets of assumed values for the model parameters. The set of values with highest probability is taken to describe the parent distribution to which the actual set of clouds in that sector belong. This is then repeated for all the sectors. In the following, we describe the model, the statistical test and the results of simulations.

Our basic model is that the spatial distribution of the local clouds can be described by a simple doughnut configuration with well defined inner and outer radii. In the present analysis, we are only concerned with its projection onto the galactic plane. The clouds are assumed to be distributed within this 'annulus' in such a manner that the areal density of clouds is a constant. Our model also assumes that the radial velocity of each cloud in the simulated population can be written as the sum of three components: (1) V_{rot} due to galactic differential rotation, appropriate to its randomly chosen location within the sector (i.e. its distance from us and its specific longitude), (2) V_{sys} due to its systematic motion, and (3) V_{pec} due to peculiar motions, assumed to have a gaussian distribution with a velocity dispersion, σ, i.e. $V_{rad} = V_{rot} + V_{sys} + V_{pec}$. The facts that the expanding ring model does not fit the molecular data in the northern sector and that the radial velocities of the local clouds show clear signature

of differential rotation suggest this assumption. Although the model is oversimplified, it is not unphysical because the values of the parameters in each sector are estimated independently. To summarize, the various parameters that enter our model are: (i) the inner and outer radii of the annulus: R_l and R_h (ii) the systematic velocity: V_{sys} (iii) the dispersion in velocity: σ.

For a particular sector, assuming a set of values for these model parameters, the positions and radial velocities of pseudo-clouds, same in number as the actual ones in that sector, are generated using Monte-Carlo simulations. The clouds are distributed at random within the longitude sector keeping the areal density constant. The radial velocity of every pseudo-cloud within this sector is assigned a rotational component arising out of galactic differential rotation, appropriate to its randomly chosen location within the sector (i.e. its distance from us and its specific longitude) and a gaussian distributed random component characterised by the chosen σ. In addition, there will be a contribution to the radial velocity due to its non-circular systematic motion, V_{sys}, also a model parameter. Thus, the radial velocity of any cloud in the simulated population is given by,

$$V_{rad}(l) = Ad \sin 2l + V_{sys} + V_{pec} \qquad (2)$$

In order to compare the observed population with the synthesised population we construct the cumulative distributions of the kinematical distances derived from their radial velocities. Kinematical distance is the hypothetical distance at which if the object is placed its radial velocity would be entirely due to galactic differential rotation. It is computed using the expression $V(l) = AD_{kin} \sin(2l)$. Next we construct a cumulative distribution of these kinematical distances i.e. $N(<D_{kin})$ vs D_{kin} for the observed and the synthesised populations. Since the number of clouds in the simulated population is rather small (typically ~ 25 in a given sector) we generate 50 realisations of the synthetic populations for a given set of values for the parameters, using a different seed number each time, and derive an 'ensemble-averaged cumulative distribution'. We then compare this' ensemble-averaged cumulative distribution of the synthetic population with the cumulative distribution of the observed population using the Kolomogorov-Smirnov test and obtain the probability that the synthetic and observed populations are drawn from the same parent distribution. As mentioned above, in obtaining the cumulative distribution for the simulated population one has assumed a particular set of values for the expansion velocity, velocity dispersion, and the distances to the inner and outer radii of the annulus in that sector. The procedure is now repeated by assuming different sets of values for these parameters.

Since there are in principle four parameters, we used a partly sequential search. To begin with, the dispersion in peculiar or random velocities (σ) was fixed at a value determined from the earlier analysis of the clouds along the four null directions. It may be recalled that the dispersion in the peculiar velocities varied from 2 to $5\,\mathrm{kms}^{-1}$ depending on the direction. The velocity dispersion for any particular sector was obtained by interpolation. The expansion velocity, inner and outer radii of the annulus as measured from the sun were varied and the cumulative distributions were compared with that of the observed sample. The best-fit distribution was identified as the one with the highest Kolomogorov-Smirnov probability. Thus, for every given longitude sector the most probable values for V_{exp}, R_l and R_h were obtained. To illustrate how sensitive the cumulative distributions are to the choice of the parameters, we have summarised the parameters and their K-S probabilities for the best and

Table 6a. Parameters for the good fits.

Longitude bins	1	2	3	4	5	6	7	8	9	10
V_{exp} (kms^{-1}) (fixed)	4.5	4.0	4.0	−3.5	−4.0	4.0	2.5	4.5	1.0	10.0
% Probability	100	100	98	100	91	92	100	100	100	100
σ (kms^{-1})	2.5	3.0	4.0	6.0	5.5	5.0	4.5	4.5	4.5	8.0
R_L (pc)	150	250	200	100	250	250	250	300	1300	110
R_H (pc)	400	500	350	450	550	550	550	650	1600	360

Table 6b. Parameters for the poorer fits.

Longitude bins	1	2	3	4	5	6	7	8	9	10
V_{exp} (kms^{-1}) (fixed)	4.5	4.0	4.0	−3.5	−4.0	4.0	2.5	4.5	1.0	10.0
% Probability	64	70	72	76	70	77	72	85	70	70
σ (kms^{-1})	4.0	4.5	6.0	8.0	7.5	7.0	6.5	6.5	6.5	8.0
R_L (pc)	200	250	100	150	200	350	300	150	1300	110
R_H (pc)	400	450	300	450	500	600	550	450	1500	260

somewhat poorer fits for each of the ten sectors in Tables 6a and 6b. For the first two sectors, we have also shown the plots of the corresponding cumulative distributions for the best and poorer fits in Fig. 6. Then, fixing the expansion velocities at the values derived above, the dispersions (σ) in the peculiar velocities, as well as R_l and R_h were varied in the next stage of simulations. This was done mainly to verify the robustness of the conclusions of the previous set of simulations. It turned out that the best fit values for the velocity dispersions agree reasonably well with the values derived earlier from the analysis of the clouds in the *null* directions and the reflection nebulae.

The variation of the K-S probabilities with respect to these parameters is not strongly peaked and therefore the derived parameters could not be estimated more accurately. In summarising the *most probable* values for the parameters in Table 7, we have ascribed errors to take this into account. Having pointed out that the distribution of probabilities has a rather broad maximum, it should also be emphasized, however, that the derived values of the parameters pass various consistency checks. For example, the most probable value for V_{exp} in the various directions derived here agree well with the values obtained from the analysis described in the previous sub-sections. Also, the derived spatial distribution of the local dark clouds projected onto the galactic plane, shown in Fig. 7, agrees well with results obtained from various other studies. This is discussed in the next section. Below, we list the main results of the detailed analysis presented in this section.

■ The population of the local dark clouds appears to be in a state of expansion about a common centre. Their radial velocity of expansion with respect to us is about 4 kms^{-1}.

■ In addition to their systematic motions (i.e. galactic rotation with a superimposed
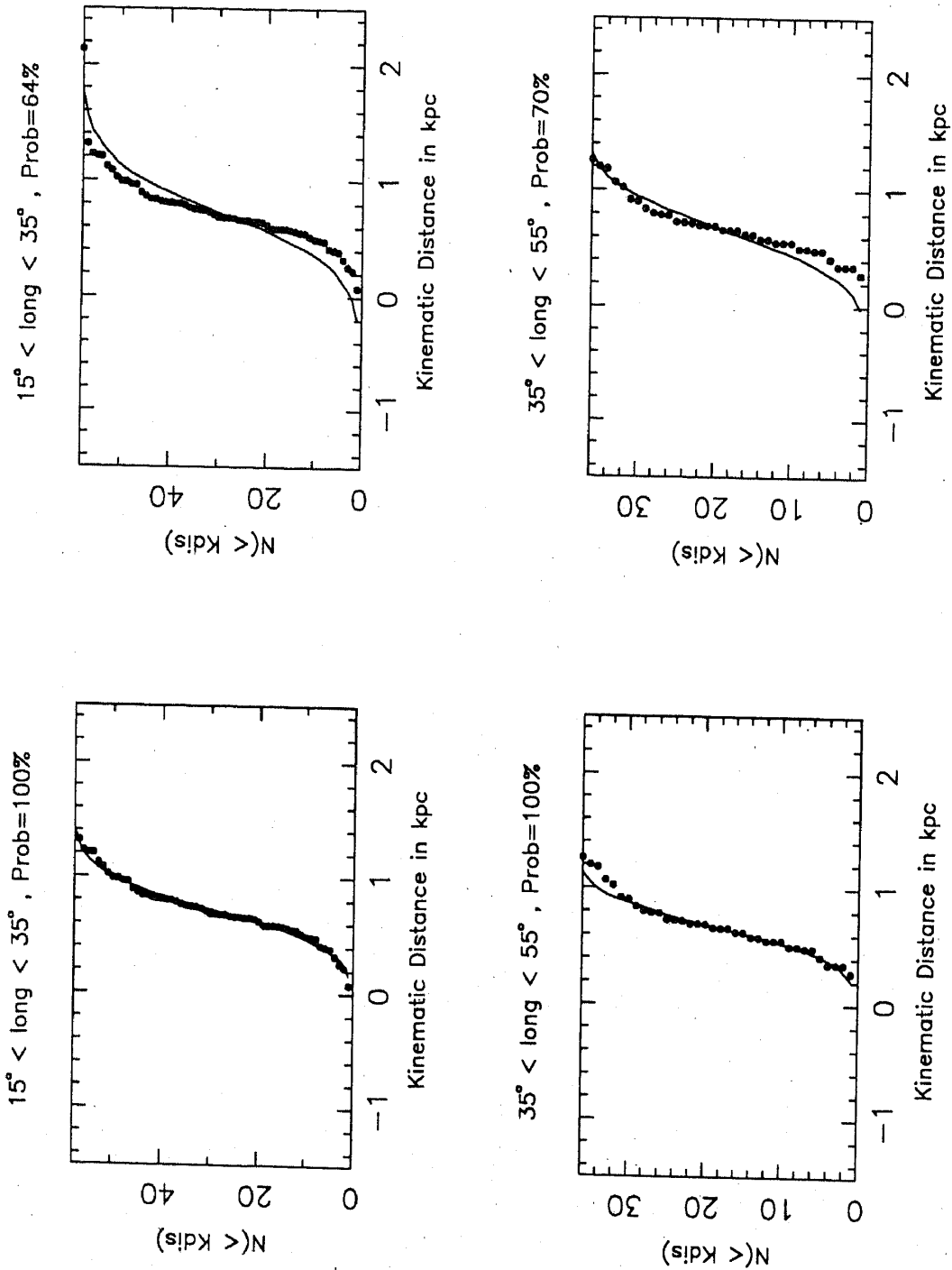
Figure 6. The top and the bottom plots show the cumulative distributions of the *kinematic distances* of the observed clouds and those of simulated populations for the longitude sectors 15°–35° and 35°–55°, respectively. The filled circles represent the observed clouds, and the continuous line is the ensemble-averaged cumulative distribution of the simulated populations. For each of the two longitude directions model fits with two different Kolomogorov-Smirnov probabilities have been shown.

Table 7. Final fit parameters.

Longitude bins	1	2	3	4	5	6	7	8	9	10
$V_{exp}(\text{kms}^{-1})$	4.5	4.0	4.0	−3.5	−4.0	4.0	2.5	4.5	1.0	10.0
$\sigma(\text{kms}^{-1})$	2.5	3.0	4.0	6.0	5.5	5.0	4.5	4.5	4.5	
$R_L(pc)$	150	200	130	150	250	250	250	300	1300	15..
$\delta R_L(pc)$	50	50	30	50	50	50	50	100	100	5..
$R_H(pc)$	400	500	400	450	550	600	550	650	1600	
$\delta R_H(pc)$	50	50	50	50	50	50	50	50	100	5..
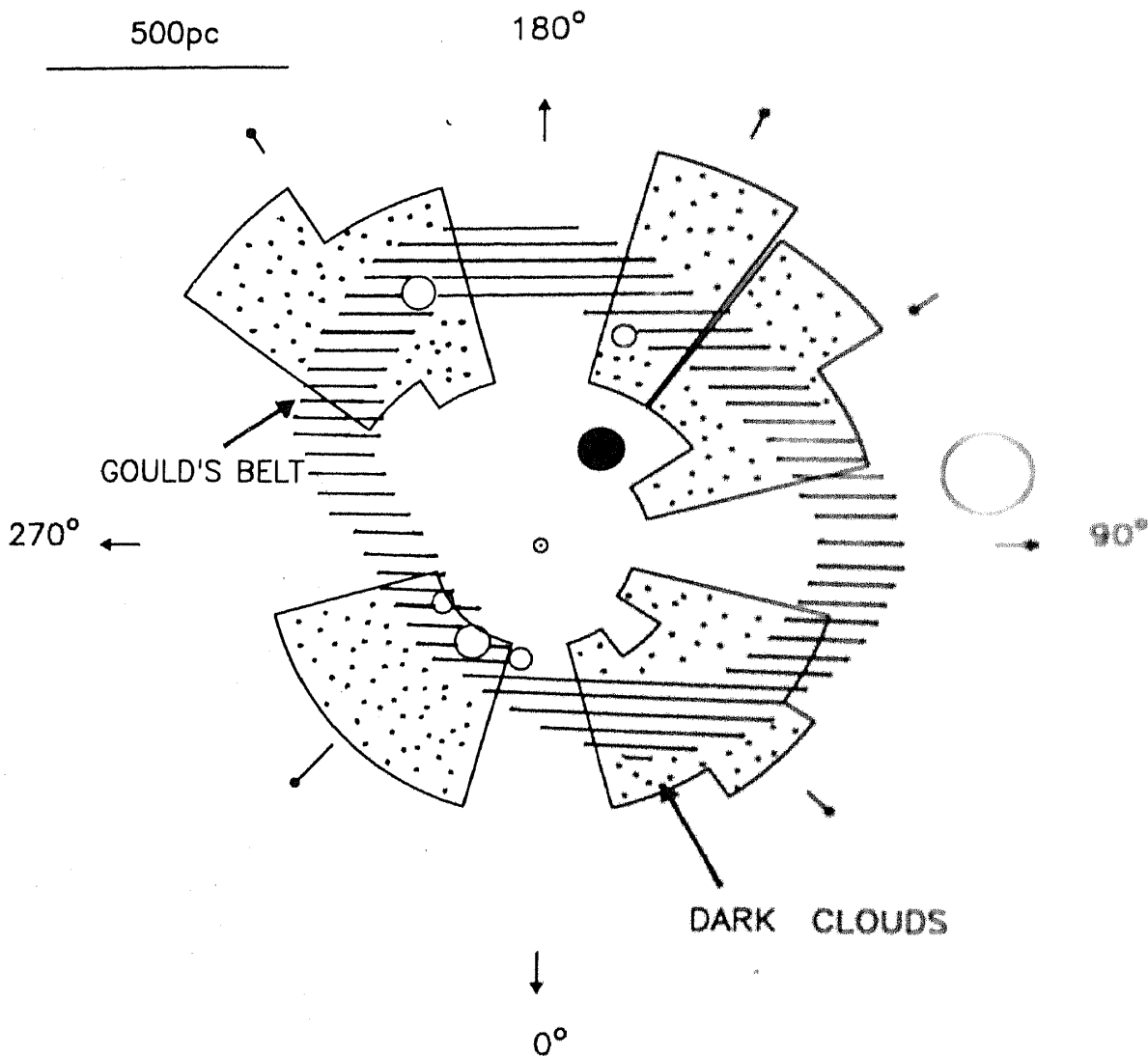
Figure 7. A schematic diagram of the projected spatial distribution of the local dark clouds derived from Table 7. The sun is located at the centre. The open circles indicate the nearby OB associations viz. Orion, Perseus, Lacertae I and Scorpio-Centaurus. The filled circle indicates the position of the Cas-Tau group. The clouds along the four *null* directions are not shown since the estimate of the mean distances to them as derived from the analysis described in section 3.3 are unreliable. The clouds in the longitude range 235°–255° are at a distance of ~ 1·4 kpc and are presumably unrelated to the local system of expanding clouds, hence they too have not been shown. For comparison, Gould's belt is shown by the hatched oval. Except for the clouds in the longitude range 105°–145° which have predominantly negative (inward) velocities, the rest of the clouds are all receding.

expansion velocity about a common centre) the clouds have peculiar or random velocities with a dispersion ~ 3 to $6\,\text{kms}^{-1}$.

■ As to their spatial distribution, a model in which they are distributed in an oval-shaped doughnut with the sun offset from the centre fits the data reasonably well. The distance to the inner edge of the doughnut varies from 150 to 300 pc, while that to the outer edge varies from 400 to 600 pc depending upon the longitude. *In our opinion the depletion of clouds in the central region is statistically significant.* A rough estimate suggests that the *morphological centre* of the population of these clouds is at a distance of ~ 160 pc from the sun towards 215° longitude. The mean radius of the doughnut from such an assumed *morphological centre* is ~ 400 pc and the *expansion age* is ~ 100 Myr.

■ In the longitude range 235° to 255°, most of the clouds in our sample appear to be unrelated to this system of expanding clouds, and are at a much greater distance of ~ 1.4 kpc. (Hence they are not shown in the schematic Fig. 7.)

■ An intriguing feature of the local population of the dark clouds is that most of the clouds in the longitude range 100° to 145° have negative radial velocities implying that they are approaching us.

4. Discussion

In this section, we discuss our results in relation with those arrived at by earlier workers and highlight the agreements and disgreements.

4.1 *Expansion*

Our finding that the local population of dark clouds are expanding is in agreement with a similar result arrived at by Taylor *et al.* (1987) from an earlier but limited study. The average expansion velocity of $\sim 4\,\text{kms}^{-1}$ derived by us is also consistent with the expansion seen in the local population of O-B stars (Oort 1927; Cameron & Torra 1990). Optical studies suggest that of the stars within ~ 600 pc only those with ages < 30 Myr show expansion; the older stars within this volume appear to be kinematically inactive. One of our results viz. that there is a depletion of molecular clouds within a distance of $\simeq 200$ pc from the *morphological centre* is consistent with this.

4.2 *Peculiar velocities*

In addition to the expansion, there is clear evidence for peculiar motions as well. The dispersion in the peculiar velocities is ~ 3 to $6\,\text{kms}^{-1}$. This is consistent with the mean absolute deviation in the peculiar velocities of the nearby OB stars as derived by Blaauw (1956). He found this quantity to be $\sim 2\,\text{kms}^{-1}$ perpendicular to the line of sight and $\sim 3\,\text{kms}^{-1}$ along the radial direction. Our values for the dispersion in different directions are likely to be a little higher because of the possible contributions due to improper distance corrections.

Stark (1984) estimates the velocity dispersion of clouds to be $\sim 8\,\text{kms}^{-1}$ from a study of molecular clouds in the anti-centre direction. This is *larger* than our estimate of 3 to $6\,\text{kms}^{-1}$ for the local dark clouds as well as a value of $5\,\text{kms}^{-1}$ derived for the

Clouds towards 180 deg.
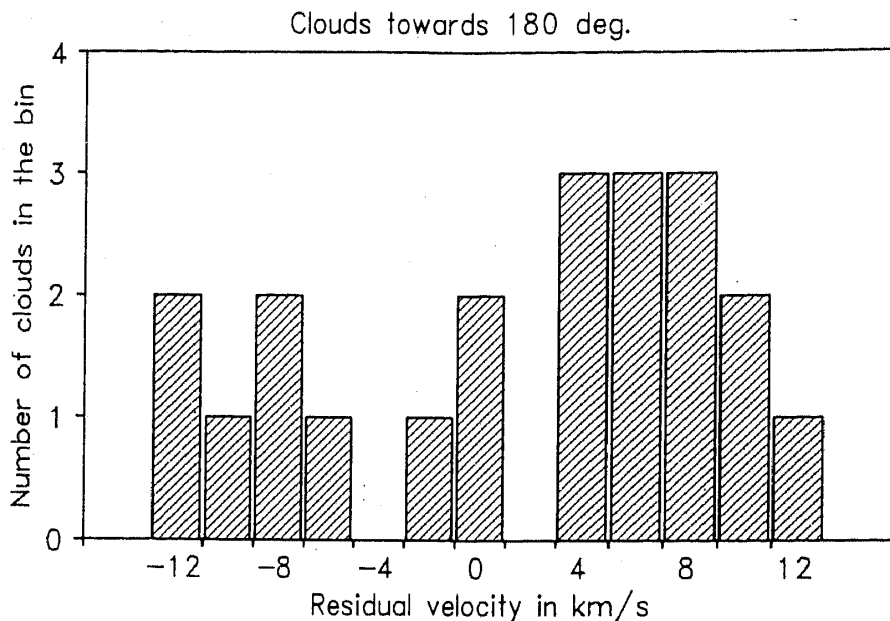
Figure 8. The histogram shows the residual velocities of clouds towards the anticentre direction observed by Stark (1984) after correcting for multiple sampling of the clouds. This was done by requiring that only one cloud occupies a *cell* of dimension 1·5° in longitude as well as latitude, and 2 km/s in velocity. At first sight, this histogram would suggest a very large velocity dispersion for the clouds, but in our opinion, this distribution may consist of more than one group of clouds. Also, any systematic velocity has to be taken out before deducing the true velocity dispersion.

HI clouds in the galactic centre direction (Radhakrishnan & Srinivasan 1980). In this study, we have removed systematic non-circular motions before calculating the dispersion, but Stark's values include such motions. In Fig. 8 we have plotted a histogram of the residual velocities of the clouds discussed by Stark (1984) after identifying distinct kinematical entities as described in the last section. Clearly it is not a *randomised* distribution. In principle, this histogram could be rationalised in terms of two distinct groups of clouds, although we have no way to prove this. Here, we merely wish to point out that the *velocity dispersion* derived from this histogram is bound to be an overestimate.

The kind of estimate made by Stark is, of course, the relevant one if one wishes to study the overall energy in non-circular cloud motions. Our estimate, by removing systematic motions as far as feasible, would correspond to a local dispersion which would be the relevant parameter for modelling the dynamics of a cloud complex i.e. estimating collisions between subclouds and providing for their *heating*.

4.3 Distribution of the local dark clouds

In Fig. 7 we have sketched the projected space distribution of the clouds as derived by us. As will be seen, the molecular clouds have a *thicker* distribution than a *thin ring* as conjectured by Lindblad *et al.* (1973). The dimensions of the HI ring in various directions are in general agreement with the inner boundary of the molecular 'annulus' and the O-B associations that define Gould's belt lie well within this annulus. The

spatial distribution is also in good agreement with the distribution of dust in the solar neighbourhood obtained from reddening measurements (Lucke 1978). It is also consistent with the extinction data along various longitudes in the solar neighbourhood. For example, it will be seen that between longitude 235° and 255° most of the dark clouds contained in our sample are at a much greater distance of ~ 1·2 kpc (and therefore not shown in the figure). This is in agreement with the low extinction in this direction upto large distances as found by Westin (1985). The rise of extinction to substantial values even at smaller distances in the first two quadrants is also consistent with smaller values for the inner radius of the annulus in these quadrants.

While the overall distribution is in accord with the optical and the HI studies, there is an important difference. We do not find any evidence for this expanding system of clouds to define a distinct plane or a slab inclined to the galactic plane. In this regard we disagree with the conclusion drawn by Taylor *et al.* (1987) that only the clouds in the Gould's belt plane show significant evidence for expansion. They separated the northern dark clouds into two populations, one belonging to Gould's belt and the other to the galactic plane, using a simple criterion based on proximity on the sky and an iterative procedure. They find that only the clouds in the Gould's belt show significant evidence for expansion. The local clouds in the galactic plane show at best only marginal evidence for expansion. Even this, they attribute to *contamination* of the galactic plane population by the clouds belonging to the Gould's belt in the cross-over directions where the separation into two populations is difficult.

In our analysis so far we have made no attempt to separate the clouds in this manner. But in order to verify this conjecture by Taylor *et al.* we separated our sample of clouds (i.e. both the northern and southern clouds) into two distinct planes or slabs following their prescription. It turns out that there are only two longitude sectors (15° − 35° and 55° − 75°) with statistically significant number of clouds belonging to each of the two subgroups (see Table 8). We subjected the clouds in these two sectors to the analysis procedure outlined in section 3·3, *but this time keeping the two populations distinct.* The comparison of the simulated cumulative distributions with the observed ones is shown in Fig. 9, and the resultant best fit parameters are given in Table 9. As can be clearly seen, *the two populations i.e. one belonging to Gould's belt plane and the other to the galactic plane show no significant differences in their kinematical behaviour or spatial distribution.* We thus conclude that the clouds in the various longitudes share similar motions regardless of which of the two hypothetical planes they are assigned to.

There are also other reasons why one might consider such a structure with age comparable to the local semi-oscillation period of 30–40 Myr to be apparent rather than real. First of all, even if a set of expanding clouds were initially confined to a thin planar ring inclined with respect to the galactic plane, with the passage of time

Table 8. Distribution of independent clouds in the various longitude bins after separating them into the Galactic and Gould's belt populations.

Longitude bins	1	2	3	4	5	6	7	8	9	10
Galactic plane	33	27	19	61	25	33	4	6	16	2
Gould's plane	25	9	18	10	0	8	22	6	0	23
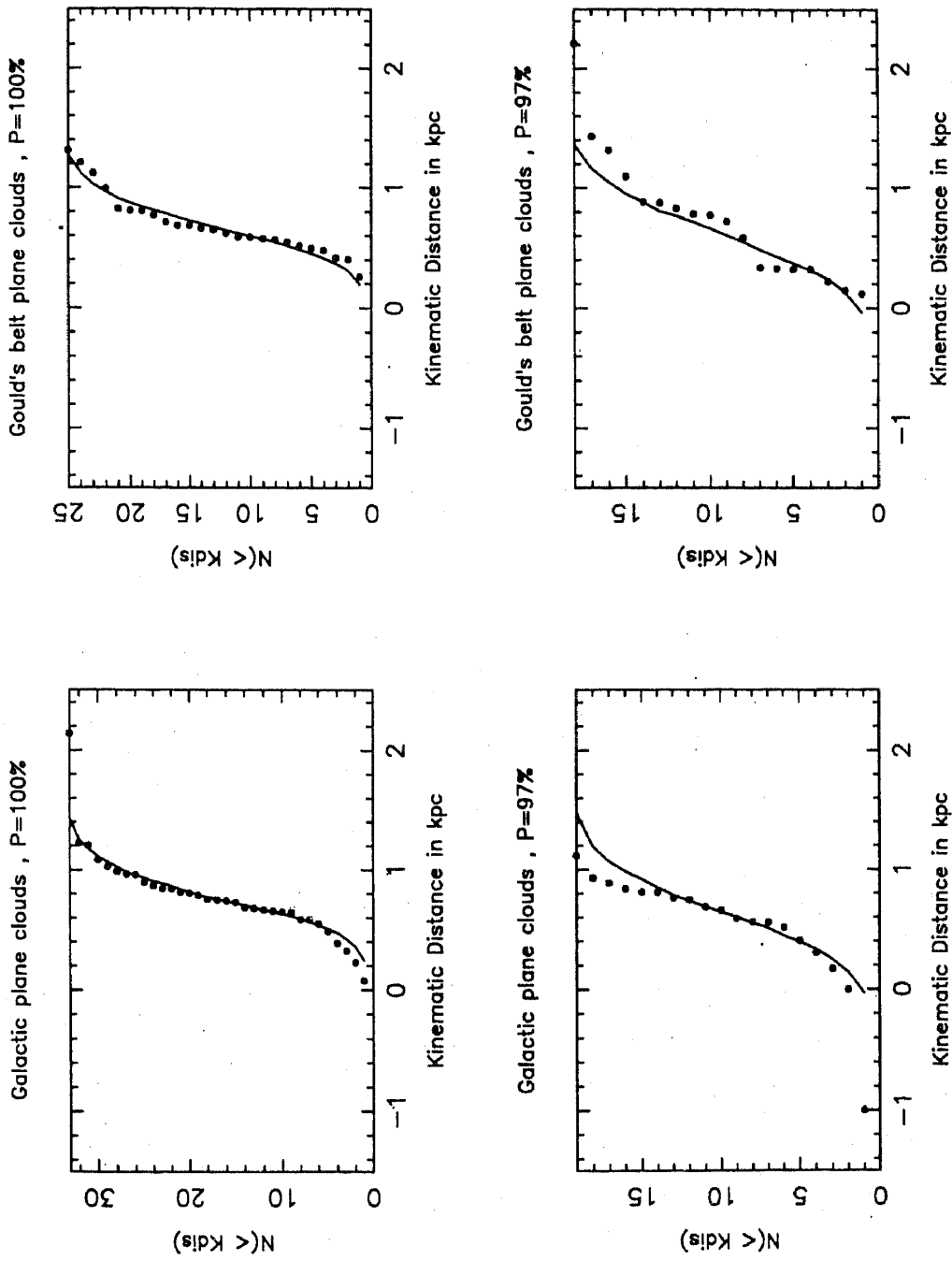
Figure 9. The cumulative distribution of the kinematic distances of the clouds in the longitude ranges 15°–35° and 55°–75°. The panels on the left are for the *galactic plane* clouds while those on the right are for the *Gould's belt plane* clouds. Our main conclusion from this is that both the *galactic plane* clouds and the *Gould's belt plane* clouds show similar kinematics.

Table 9. The best fit values of the four model parameters for the two directions: $15° \leq l \leq 35°$ and $55° \leq l \leq 75°$. Here V_{exp} is the expansion velocity, σ the velocity dispersion and R_L and R_H refer to the inner and outer radii of the spatial distribution of the dark clouds.

	V_{exp} kms^{-1}	σ kms^{-1}	R_L pc	R_H pc	V_{exp} kms^{-1}	σ kms^{-1}	R_L pc	R_H pc
Galactic plane	5.5	2.5	150	350	4.0	4.0	150	400
Gould's plane	4.0	2.5	200	400	3.5	4.0	200	400

this distribution will get smeared out and merge with the so called *galactic plane clouds* due to peculiar or random motions. Secondly, creation of such a structure seems to require extremely special conditions. It is difficult to imagine how an inclined structure can be created or if created initially in the plane how the required special distribution of the normal component of the mean velocity can be given. Any deviation from this special distribution would produce warps and wriggles along the belt as it oscillates in the local galactic potential which, given the age of 30–45 Myr, would help in further obliterating its distinct identity from the disk population.

4.4 Some dark clouds with 'anomalous' motions

As already mentioned, most of the clouds in the longitude range 100° to 145° are not receding *but coming towards us*. We have no plausible suggestions to make regarding such an apparent streaming motion. It would be worth exploring whether this is due to a velocity reversal induced by some recent stellar explosions or young associations in that region.

Another puzzling feature is the presence of the Taurus molecular clouds near the morphological centre of the expanding population of clouds that we have been considering. Although the radial component of their velocities are positive suggesting that they might be part of the expanding system, their location right near the centre of the system would contradict such an association. The Taurus molecular clouds also differ in two important ways from the Ophiucus and Orion clouds: (1) they do not show evidence of one-sided compression such as one would expect from a set of clouds expanding due to a central energy-momentum source: (2) star formation in these clouds is more or less uniformly distributed (Blaauw 1991). There are two resolutions to this dilemma: either the Taurus molecular clouds have migrated to their present location and therefore are not part of the family of expanding clouds or that they have formed more recently than the expanding system of clouds (Blaauw 1991).

4.5 Origin of the motions

Having discussed the expansion and the distribution of the local dark clouds as well as the Gould's belt system of stars, we now turn to a discussion of their possible origin. The two basic facts that need to be explained are the energy and the momentum

in the expansion of the system of stars as well as the clouds, and their presently observed morphology and the nature of their motions.

Energy and momentum: The suggestions that have been made in the literature regarding the source of the energy and momentum responsible for the expansion fall into two categories: according to one hypothesis (see Blaauw 1991 for a review), the observed expansion could be understood in terms of the continued action of the ionising radiation, stellar wind and supernovae from massive stars belonging to the *Cas-Tau* association located close to the morphological centre of the system. The one-sided star formation in the three major nearby cloud complexes – Orion, Sco-Cen and Perseus – is consistent with this idea. But the *inclination* of the Gould belt system of bright B stars is harder to explain in this picture. An alternative hypothesis due to Franco *et al.* (1988) is that the observed ring-like structure might be understood in terms of the impact of a high-velocity cloud with the galactic disk and the resultant *splash* (Elmegreen 1991). While such an exotic mechanism might explain the location of some of the nearby big molecular cloud complexes (such as Orion) at substantial distances from the galactic plane it is difficult to understand the observed expansion in this picture. In view of this, in the discussion to follow, we will assume that the *Cas-Tau* association is the more likely *central engine* which has powered the expansion. Similar expanding systems of clouds with young OB stars located in the interior – such as the systems of cometary globules and clouds found in Orion, Vela, Cepheus and Rosette regions (Bally *et al.* 1991; Sridharan 1992; Patel *et al.* 1993; Indrani & Sridharan 1994) – lend credibility to this idea. In principle, there are three mechanisms in this scenario that can supply energy and momentum to the clouds: (1) stellar winds, (2) supernovae, and (3) the rocket effect (Oort & Spitzer 1955). We shall now make simple estimates for the energy and momentum that each of these processes can contribute to see if they can meet the requirements.

The local dark clouds are found to have an average ^{13}CO column density of $\sim 60 \times 10^{14}\,cm^{-2}$. Using a $N_{^{13}CO}$ to N_{H_2} conversion factor of 5×10^5 (Dickman 1978) and assuming a mean molecular hydrogen volume density of $500\,cm^{-3}$ the estimated average sizes and masses of the clouds are $\sim 2\,pc$ and $600\,M_\odot$, respectively. We estimate that there are ~ 300 such clouds in the first two quadrants alone. Thus the total mass of these clouds would be $\gtrsim 2 \times 10^5\,M_\odot$ and for an average expansion speed of $\sim 4\,kms^{-1}$ the total energy would be $\sim 10^{50}\,erg$.

Blaauw (1991) has estimated that ~ 15 OB stars would have evaporated from *Cas-Tau* in its lifetime ($\sim 45\,Myr$). The stellar winds acting over $10\,Myr$ as well as the subsequent supernovae of massive stars inject similar amounts of mechanical energy and mass which for 10 such stars are $\sim 10^{52}\,erg$ and $\sim 100\,M_\odot$ respectively. Here we have assumed a mass loss rate of $\sim 10^{-6}\,M_\odot\,yr^{-1}$ and a wind velocity of $\sim 2000\,kms^{-1}$. If a reasonable fraction, say 10%, of this energy is intercepted by the clouds the energy requirement can be satisfied but not the momentum. This is because the momentum goes as $\sqrt{2 \times Mass \times Energy}$ and balancing the momentum in the clouds with that in the ejecta requires that the ratio of their kinetic energies is equal to the inverse of the ratio of their masses. In the above cases, while the net mass of the clouds is ~ 1000 times larger than the total ejected mass, even the maximum available mechanical energy in the ejecta is only ~ 100 times larger than that required. This disparity becomes even larger if one assumes some reasonable values for the fraction of mass and energy intercepted. Thus both the stellar winds and the super-

novae from 10 massive stars seem to be unlikely candidates as the primary energy-momentum source. However, it should be noted that a large fraction of the energy goes into *heating* up the matter and the increased internal pressure will push the clouds outward. This is possibly more effective than the direct momentum transfer in the above two mechanisms.

The third mechanism viz. the *rocket effect*, on the other hand, seems to be more probable. When a neutral gas cloud is exposed to the ionising radiation from a star, an ionisation front will be driven into the cloud. The ionised hydrogen produced on the side of the cloud facing the star is at a much higher pressure than the gas outside because of the higher density. Hence this gas expands, producing a recoil on the cloud and thus accelerating it away from the star. This process known as the *rocket effect* (Oort & Spitzer 1955) can accelerate interstellar clouds to high velocities and hence supply the required momentum. However, in the process it leads to the ablation of a significant part of the cloud as well. In fact, the sound velocity in the ionised expanding dense gas is $\sim 15\,\mathrm{kms}^{-1}$, and to accelerate a cloud to this velocity half of its initial mass has to be ionised and ablated. It is conceivable that this gas after recombination is now seen as the expanding HI ring.

Morphology and kinematics: There have been two distinct suggestions regarding the origin of the observed clouds and the OB associations:

(a) The clouds were formed due to gravitational collapse of an expanding ring of gas set in motion by the central activity.
(b) The clouds existed close to the center of activity and they were pushed by an expanding ring of gas resulting from the activity at the center.

In both these scenarios, the observed OB associations are to be understood in terms of induced star formation. But there are difficulties with both these scenarios. For example, scenario (b) is inconsistent with the fact that the molecular clouds and associations are located *outside* the expanding HI ring. One would have expected the clouds to have lagged behind the expanding ring which set them in motion. From a kinematical point of view neither of the scenarios mentioned above are able to provide a satisfactory explanation for the observed radial velocities. As already remarked, Taylor *et al.* (1987) had concluded from their analysis that a model in which a ring of clouds expands from a point getting only sheared by the galactic rotation effects in the process does not fit the observed radial velocities of the northern dark clouds. Our analysis of the combined data of both the northern and southern clouds confirms this. As pointed out by Frogel & Stothers (1977) from limited data, the longitude-radial velocity plot (Fig. 1b) clearly shows a double sinewave behaviour characteristic of galactic differential rotation. The peculiar velocities as well as the distribution of clouds having finite radial thickness can cause the observed scatter. Nevertheless the local dark clouds clearly show an expansion of $\sim 4\,\mathrm{kms}^{-1}$ as well. Thus, only a model in which the clouds are participating in galactic rotation appropriate to their *present* locations, with a small expansion also super-imposed seems to fit the molecular data. This is at variance with the expanding ring model of Lindblad *et al.* (1973) mentioned above that fits well the velocity data on the local HI gas.

If we were to accept our model to describe the kinematics of the local dark clouds, then it is quite clear that cloud–cloud encounters must be an important ingredient

of any scenario. In this regard, we wish to advance the following suggestion. Let us assume that the *Cas-Tau* group of stars formed in a giant molecular cloud. Due to stellar winds and ultraviolet radiation from the massive stars as well as supernova activity, the parent cloud would have fragmented: the denser fragments would have been accelerated through, say, the *rocket effect* (Oort & Spitzer 1955), and in the more diffuse regions the molecular gas would have been dissociated and perhaps even ionised. Due to the continuing action of the stellar winds from the association a large cavity would have been excavated with the more diffuse gas swept into an expanding shell. As the local dark clouds in the vicinity were overtaken by this expanding shell of swept-up gas they too would have been set in motion due to the combined effect of the *Cas-Tau* group of stars and also possibly due to the interaction between the expanding shell of gas and the dark clouds. It is entirely conceivable that during the subsequent 30 to 40 Myr the systematic motions of these clouds could have been degraded through collisions with other clouds in the surrounding interstellar medium. Provided these collisions are sufficient in number, one would expect that the galactic rotational effects would eventually become more important than expansion.

We present a simple estimate to support this conjecture. Let us assume that due to the combined effects of ultraviolet radiation and stellar winds a certain number of clouds are accelerated to a velocity of, say, $\sim 20 \, \mathrm{km s}^{-1}$ which is comparable to the sound speed in the ionised front of the clouds (Spitzer 1978). Let M_1 be the combined mass of these clouds and M_2 be the total mass of the interstellar clouds to which they have imparted energy and momentum. Thus $M_1 + M_2$ will be the mass of the clouds in the doughnut shaped configuration expanding radially with a velocity of $\sim 4 \, \mathrm{km s}^{-1}$.

Momentum conservation requires $(M_1 + M_2) V_2 = M_1 V_1$. For the assumed values of $V_1 \sim 20 \, \mathrm{km s}^{-1}$, $V_2 \sim 4 \, \mathrm{km s}^{-1}$, this implies that $M_2/M_1 \sim 4$. An inspection of Fig. 7 displaying our derived distribution of the system of expanding clouds shows that the ratio of the projected area of the annulus to that of the centrally depleted region is ~ 5 to 6. Thus the expectation that a certain number of clouds initially accelerated by the *Cas-Tau* group of stars could have imparted radial motions to the remaining clouds is consistent with our derived distribution. Or to put it differently, it is not too difficult to account for the energy and momentum of the system of clouds.

A more arguable point is the following: Does one expect a sufficient number of cloud–cloud collisions to have taken place during the last 30 Myr or so to erase the initial signature of uniform expansion from a common centre? For this to be true the effective cross section for cloud–cloud collisions must be greater than a minimum value given by

$$\sigma_{min} \sim \frac{a^3}{Vt} \tag{3}$$

where a is the mean separation between the clouds, V the relative velocity and t the age of the system. From the geometry of the distribution of clouds given in Fig. 7 and the total number of clouds in the sample we estimate the mean separation to be $\sim 60 \, \mathrm{pc}$. For an assumed value of $V \sim 20 \, \mathrm{km s}^{-1}$ and $t \sim 30 \, \mathrm{Myr}$, the effective cross section must be $\geqslant 225 \, \mathrm{pc}^2$ in order for collisions to be important. In other words, the *effective sizes* of the clouds must be $\sim 15 \, \mathrm{pc}$. Interestingly this is only 3 to 5 times

B. Ramesh

the mean sizes of the clouds. Thus the importance of cloud–cloud collisions possibly mediated by galactic magnetic fields cannot *a priori* be ruled out (see Elmegreen 1987a, b for a relevant discussion). A detailed investigation of this important and interesting question may be worthwhile but is beyond the scope of this paper. We merely wish to point out the difficulty in understanding the kinematics of the local dark clouds without invoking cloud–cloud collision.

5. Summary

We shall now summarise our main findings. Our objective was to study the kinematics and the spatial distribution of the local dark clouds. Towards this aim the radial velocities towards 115 southern dark clouds were obtained using the $J = 1 \rightarrow 0$ transition of ^{12}CO. Using different methods we analysed these velocities along with those of the northern dark clouds obtained by Taylor *et al.* (1987). We agree with their conclusion that the kinematics of the local clouds is not describable by the expanding ring model proposed for the local HI gas. We find that the observed distribution of the radial velocities is best understood in terms of a model in which the local clouds are participating in circular rotation appropriate to their present positions with a small expansion also super-imposed. This possibly implies that cloud–cloud collisions are important. The $4 \, kms^{-1}$ general expansion as well as the spatial distribution derived are in good agreement with those obtained from optical studies. This includes the finding that clouds in the longitude range 235° to 255° are unrelated to the system of expanding clouds, and are at a much greater distance of $\sim 1\cdot4 \, kpc$. Intriguingly, most of the clouds in the longitude range 100° to 145°, and some in the range 195° to 215°, appear to have negative radial velocities implying that they are approaching us. The reason for such a streaming motion of a subset of clouds is not clear.

Acknowledgements

References

Bally, J., Langer, W. D., Wilson, R. W., Stark, A. A., Pound, M. W. 1991, in *IAU Symp. No. 147 on Fragmentation of Molecular Clouds and Star Formation*, Eds. E. Falgarone, F. Boulanger & G. Duvert, (Dordrecht: Kluwer) p. 11.
Blaauw, A. 1991, in *The physics of star formation and the early stellar evolution*, Eds. C. J. Lada & N. D. Kylafis (Kluwer Academic Publ.) p. 125.

Blaauw, A. 1956, *Astrophys. J.*, **123**, 408.

Cameron, F., Torra, J. 1990, *Astr. Astrophys.*, **241**, 57.

Dame, T. M., Ungrechts, H., Cohen, R. S., de Geus, E. J., Grenier, I. A., May, J., Murphy, D. C., Nyman, L. A., Thaddeus, P. 1987, *Astrophys. J.*, **322**, 706.

de Vries, C. P., Brand, J., Israel, F. P., de Graauw, Th., Wouterloot, J. G. A., van de Stadt, H., Habing, H. J. 1984, *Astr. Astrophys. Suppl.*, **56**, 333.

Dickman, R. L. 1978, *Astrophys. J. Suppl.*, **37**, 407.

Elmegreen, B. G. 1991, in *The galactic interstellar medium* Eds. W. B. Burton, B. G. Elmegreen & R. Genzel (Saas-Fee advanced course 21), 164.

Elmegreen, B. G. 1987a, in *Physical Processes in Interstellar Clouds*, Eds. G. E. Norfill & M. Scholer (NATO ASI C Series Vol. 21), 1.

Elmegreen, B. G. 1987b, in *Physical Processes in Interstellar Clouds*, Eds, G. E. Norfill & M. Scholer (NATO ASI C Series Vol. 21), 105.

Feitzinger, J. V., Stuwe, J. A. 1984, *Astr. Astrophys. Suppl.*, **58**, 365.

Feitzinger, J. V., Stuwe, J. A. 1986, *Astrophys. J.*, **305**, 534.

Franco, J., Tenario-Tagle, G., Bodenheimer, P., Rosyczka, M., Mirabel, I. F. 1988, *Astrophys. J.*, **333**, 826.

Frogel, J. A., Stothers, R. 1977, *Astr. J.*, **82**, 890.

Indrani, C., Sridharan, T. K. 1994, *J. Astrophys. Astr.* **15**, 157.

Kerr, F. J., Bowers, P. F., Hendrson, A. P. 1981, *Astr. Astrophys. Suppl.*, **44**, 63.

Kutner, M. L., Machnik, D. E., Tucker, K. D., Dickman, R. L. 1980, *Astrophys. J.*, **237**, 734.

Kwan, J. 1979, *Astrophys J.*, **229**, 567.

Lucke, P. B. 1978, *Astr. Astrophys.*, **64**, 367.

Lindblad, P. O., Grape, K., Sandqvist, Aa., Schober, J. 1973, *Astr. Astrophys.*, **24**, 309.

May, J., Murphy, D. C., Thaddeus, P. 1988, *Astr. Astrophys. Suppl.*, **73**, 51.

Olano, C. A. 1982, *Astr. Astrophys.*, **112**, 195.

Oort, J. H. 1927, *Bull. Astr. Inst. Netherlands*, **3**, 275.

Oort, J. H., Spitzer, L. 1955, *Astrophys. J.*, **121**, 6.

Patel, N. A. 1990, Ph. D. thesis, Indian Institute of Science, Bangalore.

Patel, N. A., Xie, T., Goldsmith, P. F. 1993, *Astrophys. J.*, **413**, 593.

Racine, R. 1968, *Astr. J.*, **73**, 223.

Radhakrishnan, V., Srinivasan G. 1980, *J. Astrophys. Astr.*, **1**, 47.

Sahu, M. S. 1992, Ph.D. Thesis, University of Groningen.

Spitzer, L., Schwarzschild, M. 1951, *Astrophys. J.*, **114**, 385.

Spitzer, L. 1978, in *Physical processes in the interstellar medium* (New York: Wiley), pp. 227.

Sridharan, T. K. 1992, *J. Astrophys. Astr.*, **13**, 217.

Stark, A. A. 1984, *Astrophys. J.*, **281**, 624.

Stark, A. A., Blitz, L. 1978, *Astrophys. J. (Lett)*, **225**, L15.

Taylor, D. K., Dickman, R. L., Scoville, N. Z. 1987, *Astrophys. J.*, **315**, 104.

van den Bergh, S., Herbst, W. 1975, *Astr. J.*, **80**, 208.

Westin, T. N. G. 1985, *Astr. Astrophys. Suppl.*, **60**, 99.